J. Am. Soc. Mass Spectrom. (2017) 28:119–124
DOI: 10.1007/s13361-016-1509-7

RESEARCH ARTICLE

Increased Ion Transmission for Differential Ion Mobility Combined with Mass Spectrometry by Implementation of a Flared Inlet Capillary

Matthew T. Campbell, Gary L. Glish

Department of Chemistry, Caudill Laboratories, The University of North Carolina at Chapel Hill, Chapel Hill, NC 27599-3290, USA

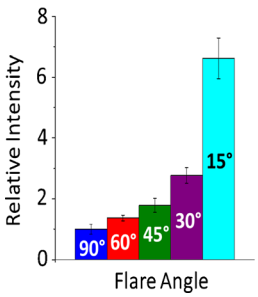

Abstract. Differential ion mobility spectrometry (DIMS) is capable of separating components of complex mixtures prior to mass spectrometric analysis, thereby increasing signal-to-noise and signal-to-background ratios on millisecond timescales. However, adding a DIMS device to the front end of a mass spectrometer can reduce the signal intensity of subsequent mass spectrometric analysis. This is a result, in part, of ions lost due to inefficient transfer of ions from the DIMS device through the aperture leading into the mass spectrometer. This problem of transferring ions can be at least partially corrected by modifying the front end of the inlet capillary leading to the vacuum of the mass spectrometer. The inner diameter of the ion-sampling end of the inlet capillary was enlarged by drilling into the face. This results in a conical flare at the front end of the capillary, while the other end of the capillary remains unmodified. These flared capillaries allow for a greater number of ions from the DIMS device to be sampled relative to the unmodified standard capillary. Four flare dimensions were tested, differing by the angle between the wall of the flare and the outer wall of the inlet capillary. All flared capillaries showed greater signal intensity than the standard capillary with a DIMS device present without reducing the resolving power. It was also observed that the signal intensity increased as the flare angle decreased. The flared capillary with the smallest flare angle showed greater than a fivefold increase in signal intensity compared with the standard capillary.

Keywords: Ion mobility, Ion transmission

Received: 3 July 2016/Revised: 28 August 2016/Accepted: 14 September 2016/Published Online: 17 October 2016

Introduction

Mass spectrometry is an extremely selective technique that separates ions by their mass-to-charge ratio, but additional separation methods are still helpful for analyzing complex mixtures and distinguishing isobaric/isomeric compounds. Post-ionization separation techniques include ion mobility techniques such as drift tube ion mobility spectrometry (DTIMS), which separates ions on millisecond timescales. With DTIMS, ions are accelerated through a drift tube by a constant electric field. While the electric field accelerates ions, they are slowed by collisions with gas molecules in the drift tube. The time it takes an ion to traverse the drift tube is dependent on collisional cross of the ion for a given drift gas and electric field [1]. Trapped ion mobility spectrometry (TIMS) and traveling wave ion mobility spectrometry (TWIMS) are similar to DTIMS because the separation method is based upon the collisional cross-section of the ions. In all these cases the separation occurs in time [2].

These ion mobility techniques separate ions at low electric fields (<10,000 V/cm), where an ion's mobility, K, is independent of electric field strength [2, 3]. However, at electric field strengths greater than approximately 10,000 V/cm, K begins to change as a function of electric field strength. Differential ion mobility spectrometry (DIMS) is more orthogonal to other ion mobility techniques because DIMS separates ions based on differences in their high- and low-field mobilities (K_H and K_L, respectively) instead of collisional cross-sections [4–6]. Additionally, the separation occurs in space meaning that DIMS passes a continuous beam of ions through the device and can be coupled with any mass analyzer. This is advantageous over the low electric field forms of ion mobility and their separation in-time, which is only compatible with time-of-flight mass analyzers.

A DIMS device consists of two electrodes typically separated by a distance of 0.3 to 3.0 mm [7–11], though smaller gap

Correspondence to: Gary L. Glish; *e-mail:* glish@unc.edu

sizes are used on microfabricated devices [12]. Ions enter between the electrodes and are carried from the entrance to the exit of the DIMS device by a carrier gas. An asymmetric waveform is applied to the capacitively coupled electrodes generating an electric field orthogonal to the direction of ion motion into the mass spectrometer. This electric field, referred to as a dispersion field (E_D), alternates between a short time period of high electric field strength and longer time period of low electric field strength and opposite polarity on a microsecond timescale [13].

The theory describing DIMS separations has been previsoulsy described [14–19], and is breifly summarized here. When the electric field is applied, ions move towards one electrode during the low electric field portion of the waveform and towards the other electrode during the high electric field portion. The distance an ion travels during the low electric field portion (d_L) is the product of ion's low electric field mobility (K_L), the magnitude of the low electric field (E_L), and the time the low electric field is applied (t_L). Analogously, the distance an ion travels in the high electric field portion (d_H) is the product of the high electric field mobility (K_H), the magnitude of the high electric field (E_H), and the time the high electric field is applied (t_H). The asymmetric waveform is created such that $E_L(t_L) = E_H(t_H)$. Therefore, the difference of the distances moved in the high field and the low field portions are proportional to the difference in the high and low field mobilities ($d_H - d_L \propto K_H - K_L$) [1, 2, 4]. Separation occurs because ions that have a non-zero net displacement during one cycle of the waveform in the dimension of the electric field will ultimately be neutralized upon impact with an electrode, whereas ions with a net displacement of zero will successfully traverse the DIMS device. The difference in K_H and K_L for a given ion is termed the differential ion mobility. Therefore, ions that do not have the same differential ion mobility for a given E_D can be separated in space with a DIMS device.

Ions with a non-zero differential ion mobility can be passed through the DIMS device by application of dc compensation field (E_C) to one electrode. Using the E_C allows for DIMS separations to be more versatile than other ion mobility techniques that separate in time. If the E_C is scanned over a range, the differential ion mobility required to traverse the DIMS changes, allowing for a survey of the entire sample analogous to a chromatography-MS experiment. Additionally, the E_C can be held constant, allowing for a continuous beam of only ions with the required differential ion mobility similar to single ion monitoring [14].

The E_D is applied across two planar electrodes held apart by a short distance. This gap between the two electrodes forms the height of the sampling slit of the DIMS device. The width of this sampling slit is defined by the width of the planar electrodes and is typically 1 to 10 mm in non-microfabricated DIMS devices [7–9, 20, 21]. While E_D and E_C control the motion of the ions in the height dimension of the sampling slit, ions move in the direction of the width of the sampling slit by diffusion. An electrospray emitter, operated at flow rates of 1–20 μL/min, can produce a spray plume wider than the width of sampling slit [22], and ions will enter across the entire width of the sampling slit [23, 24]. The total area of the sampling slit, defined by the distance between the electrodes and the width of the electrodes is typically 1–10 mm^2. This is much larger than the area of the aperture leading into the vacuum of the mass spectrometer, which is typically about 0.2–0.6 mm in diameter [25, 26]. Because ions are present along the entire area of the DIMS device, only a fraction will enter the smaller area aperture leading to the mass spectrometer, thereby decreasing signal intensity.

Efforts to reduce the loss in signal intensity when using a DIMS device include using inlet capillaries with a larger inner diameter. This results in increased ion transmission and signal intensity. However, increasing the inner diameter of the capillary also changes the conductance of gas into the high vacuum of the instrument, and therefore the linear flow rate of carrier gas through the DIMS device increases. Because the carrier gas is responsible for moving the ions through the DIMS device, the flow rate of the carrier gas determines the residence time for ions in the DIMS device. The resolution obtainable with a planar DIMS device increases with the square of the residence time in the DIMS device [27]. Therefore, while larger inner diameter capillaries enhance signal intensity, they also lower the maximum obtainable resolution for a given analysis. Improved ion transmission was observed when the conductance limit aperture was modified to match the planar gap. The ions traveling through a planar gap will not be confined to a circular beam. A rectangular aperture more efficiently transmits the ion beam exiting the DIMS device, showing at least a factor of 2.5 increase in ion transmission [28]. However, that is not an option on many mass spectrometers, especially if they use a capillary interface. Another solution is to shorten the length of the planar electrodes, which increases transmission at the cost of shortening residence time in the DIMS device and, thereby, decreasing separation capacity [27, 29, 30].

Here we present the effects of flaring the inner-diameter of only the ion-sampling end of the inlet capillary to increase the sampling area. Four flare dimensions were tested, differing by the angle between the wall of the conical flare and the outer wall of the inlet capillary. Signal intensity was measured while using DIMS followed by each of the flared capillaries and was compared with using DIMS followed by a standard capillary. The position of the ESI emitter was also changed relative to the inlet capillary to test if the flared capillaries retain greater signal intensity as the emitter is moved from the optimum position.

Experimental

Methanol (Optima grade), water (Optima grade), and acetic acid (ACS plus) were purchased from Fisher Scientific (Fairlawn, NJ, USA). Lysozyme from chicken egg white and ubiquitin from bovine red blood cells (min. 90% by SDS PAGE) were purchased from Sigma Aldrich (St. Louis, MO, USA) and diluted in 50/49/1 (v/v/v) methanol/water/acetic acid to a final concentration of 5 and 6 μM, respectively. A Bruker

Esquire 3000 ion trap mass spectrometer was used for all experiments. Samples were ionized with electrospray via direct infusion at 2.0 μL/min with 2.50 kV applied to the electrospray emitter while the inlet capillary was electrically grounded. The electrospray ionization desolvation gas temperature and flow rate were set to 300 °C and 5.0 L/min, respectively, in the instrument control software.

A custom-built planar DIMS device was used for all experiments. The stainless steel 6 × 25 mm electrodes are positioned 0.5 mm apart in the dimension of the applied electric field and 6 mm in the field-free dimension giving a total sampling area of 3.0 mm^2. The vespel holding the electrodes has an o-ring that creates an airtight seal over the inlet capillary to the mass spectrometer. A stainless steel housing surrounding the vespel of the DIMS device threads onto the Apollo I source of the Bruker Esquire 3000, replacing the spray shield. The opening at the end of the DIMS housing where the ions enter is the same size as in the spray shield, which is about the diameter of the capillary. When the DIMS device is mounted, the electrodes are oriented vertically. Experimental results were found not to differ based on horizontal or vertical orientation of the DIMS electrodes. The desolvation gas from the Apollo I source is rerouted through the DIMS housing to serve as both the desolvation gas and DIMS carrier gas. A custom-built power supply (Ridgeway et al., in preparation) was used to apply both dispersion and compensation fields. This power supply creates two separate sinusoidal waveforms at 1.7 and 3.4 MHz. One waveform was applied to each electrode of the DIMS device, which capacitively couple to create the necessary bisinusoidal asymmetric waveform (form factor = 0.67) [31]. A LabVIEW program was used to control the applied compensation voltage (E_C). Software allows for E_C to be scanned in any arbitrary function between –800 to +800 V/cm or held at a constant field.

For some experiments, the DIMS device was operated in a "transparent mode" (both electrodes held at ground potential). This mode of operation allows a conventional mass spectrum to be obtained without removing the DIMS device. Obviously, being able to obtain a conventional mass spectrum with DIMS in place is a very important capability. For transparent mode experiments with lysozyme, the signal intensity for the only four observed charge states (8+, 9+, 10+, and 11+) was summed because no separation occurs. For experiments where an E_D was applied, the magnitude of the compensation field was chosen separately for each E_D by first scanning the compensation field and observing the changing signal intensity for the 10+ charge state of lysozyme. The compensation field was then held constant at the magnitude where the greatest signal intensity was observed. This compensation field with maximum signal intensity was found to be the same for all capillaries at each E_D. Because separation of the four charge states was achieved with a dispersion field applied, only the signal intensity for a single charge state was used for analysis. The 10+ charge state is reported here because it was the most abundant charge state, and analyzing only the 9+ or 11+ charge states resulted in a similar trend. Full width at half-maximum measurements were made with Microcal Origin 6.0 by first fitting the data with Gaussian curves.

Modified capillaries were constructed from the standard inlet capillary for a Bruker Esquire 3000 (Figure 1). The standard inlet capillary is cylindrical, 180 mm in length, with an outer dimeter of 6.58 mm and an inner diameter of 0.50 mm. Both ends of the capillary have a metal coating where voltage can be applied. A conical flare was created by drilling through the metal coating and into the glass of the ion-sampling end of each capillary. The freshly drilled surface was then metalized to match the metal coatings on both ends of the capillaries. Ultimately, the outer diameter, total length, and inner diameter (beyond the drilled flare) of each flared capillary remained the same as the standard capillary. Four different flares were tested with flare angles of 15°, 30°, 45°, and 60°. The flare angle is defined as the angle between the edge of the flare and the outermost wall of the capillary. The standard capillary is 90° by the same definition. Smaller flare angles were not constructed because of limitations in drilling to the appropriate depth in the face of capillaries [32].

Experiments were also conducted to test if the flared capillaries retain maximum signal intensity more efficiently than the standard capillary as the ESI emitter is moved from the optimal spray position. To modify the position of the ESI emitter systematically, a three-axis stage was constructed and mounted to the top of the source housing of the mass spectrometer. The XY plane was parallel to the face of the DIMS device with the X-axis describing distance left or right across the face of the DIMS, and the Y-axis describing distance from bottom to top of the DIMS device. The Z-axis was defined as the dimension going towards and away from the DIMS device. This system was used to measure the displacement of the emitter from the optimum position. The optimum position (at X, Y, Z = 0, 0, 0) was defined as the position where the maximum signal intensity is observed. This position, with the spray tip of the ESI emitter centered with the top of the sampling slit of the DIMS device and offset 4.0 mm in the Z-axis from the sampling slit, was the same for all capillaries studied.

Results

Drilling into the ion-sampling end of the capillary to create the flared capillaries increased the sampling area from the standard

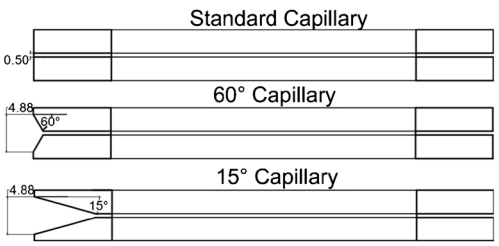

Figure 1. Cross-sections for the standard, 60°, and 15° capillaries. The schematic is drawn to scale (in millimeters) except the length of the capillaries, which has been reduced by a factor of 3. The darker lines on the two ends of the capillaries represent a metal coating, and the remaining middle portion of each capillary is glass

0.20 mm^2 to 18.7 mm^2 for all flare angles. The signal intensity for each flare angle was compared as the emitter was moved step-wise from the optimum position. For all experiments where the emitter position is changed, DIMS was in transparent mode. The emitter position was stepped from left to right (denoted the X-axis) across the face of the DIMS device in 1.00 mm increments while not changing the emitter distance from the DIMS device. After each step, the signal intensity for the four observed charge states of lysozyme was measured and summed. All signal intensities were plotted relative to the standard capillary in the optimum position, and all error bars show plus or minus one standard deviation. It was observed that all flared capillaries gave greater signal intensity than the standard capillary. Also, decreasing the angle of the flare results in an increase in the measured signal intensity. At the optimal position, the measured signal intensity increases on average by a factor of 5.3 for the 15° capillary, 3.0 for the 30° capillary, 2.3 for the 45° capillary, and 1.2 for the 60° capillary compared with the standard capillary, with no change in the average charge state within experimental error.

The three-stage axis was also used to increment the emitter position away from the inlet (denoted the Z-axis) in 0.50 mm steps while remaining in the optimum position in the X and Y axes. The signal intensity was recorded at each interval in the same manner as the experiment where the emitter was moved across the X-axis. Again, all flared capillaries show greater signal intensity than the standard capillary at all positions, and the measured signal intensity increases as the flare angle decreases. While scanning the Z-axis the signal intensity observed with the 15° capillary increased by a factor of 6.5 compared with the standard capillary. The difference between this and the factor of 5.3 increase in signal intensity seen scanning the X-axis is attributed to experimental variation. To change out the inlet capillary, both the source and the high vacuum region of the mass spectrometer must be vented and subsequently evacuated. This is likely responsible for the small variations in relative gain of signal intensity between different experiments.

Experiments were also conducted to observe if flared capillaries retain a higher percentage of maximum signal intensity as the emitter is moved from the optimal position than the standard capillary. The signal intensity was measured as the emitter position was systematically changed on both the X- and Z-axes while the DIMS device was again operated in transparent mode. The X-axis was scanned (in 1.00 mm intervals) at each of several positions on the Z-axis (stepped in 0.50 mm intervals). In this way, the signal intensity was measured at several positions in a plane in front of the DIMS device, and the data is plotted in a heat map (Figure 2).

Because the 15° capillary shows the greatest signal intensity, only the 15° capillary was compared with the standard capillary in this experiment. The top two plots in Figure 2 are plotted on the same absolute intensity scale with 100 being the signal intensity for the 15° capillary in the optimal position (coordinates {0, 0} in the left plot). The 15° capillary gives greater signal intensity than the standard capillary at all positions as expected. The two bottom plots of heat maps in Figure 2 are plotted in relative intensity where 100 for each plot is at the optimal position for that specific capillary. In the bottom row of Figure 2 there is very little difference between the two heat maps. Thus, the 15° capillary gives greater absolute signal intensity than the standard capillary, but it does not retain a higher percentage of its maximum signal intensity as the emitter is moved. Therefore, emitter position is equally important for the flared capillaries as the standard capillary.

If the added flare increased the conductance, increased ion transmission would be observed at the cost of lowering the potential resolving power of the DIMS device. It was observed that the vacuum pressure was unchanged after switching capillaries and allowing sufficient time for the instrument to pump down. The pressure of the fore region of the mass spectrometer displayed in the instrument control software achieved a minimum pressure of 3.26 mbar for all capillaries. This pressure gauge is sensitive enough to detect the difference in pressure if the dry gas (which heats the inlet) is changed from 300 to 200 °C, changing the fore pressure from 3.26 mbar to 3.38 mbar.

To further test that the mechanism for signal enhancement was not attributable to a change in conductance, the flared capillaries were inserted backwards into the Apollo I source. Since the flared capillaries were constructed from standard capillaries and modified on only one side, the unmodified end remains identical to the standard capillary. Therefore, when a flared capillary is inserted backwards in the source, the ion-sampling end is identical to the ion-sampling end of the standard capillary. In the case of the 15°, the emitter was scanned along the X-axis as described previously, and the DIMS device was operated in a transparent mode. The capillary was then removed and reinserted backwards into the source of the mass spectrometer. The signal intensity measured with the 15° capillary backwards was much lower than with the flared end facing atmosphere and is not statistically different from the signal intensity measured for the same experiment with the standard capillary. An analogous experiment was conducted with the 45° capillary, but the emitter was scanned along the Z-axis. As was expected, the gain in signal intensity is no longer observed for the 45° capillary when inserted backwards into the source, and the signal intensity measured with the backwards 45° capillary is not significantly different from the standard capillary.

To ensure that the separation achievable with the DIMS device was unchanged by the different capillaries, an E_D of 40.0 kV/cm was applied to the DIMS device. Ubiquitin was ionized with ESI from the optimal position. The compensation field was then scanned in 2.0 V/cm steps, and the full width at half-maximum (FWHM) were measured for the resulting peaks of the +8 (m/z 1072) and +12 (m/z 715) charge states of ubiquitin. These charge states were selected because they gave the most Gaussian shaped peaks of the charge states observed in the mass spectra. Deviation from a Gaussian shaped peak is a result of incomplete separation of multiple conformations of a single charge state. The FWHM were compared between the 15° capillary and the standard capillary. The FWHM observed for both charge states (within a standard deviation) does not differ significantly. Thus, the separation achievable with the DIMS device is independent of the type of capillary used. The signal intensity measured for the five different capillaries was also compared while applying a

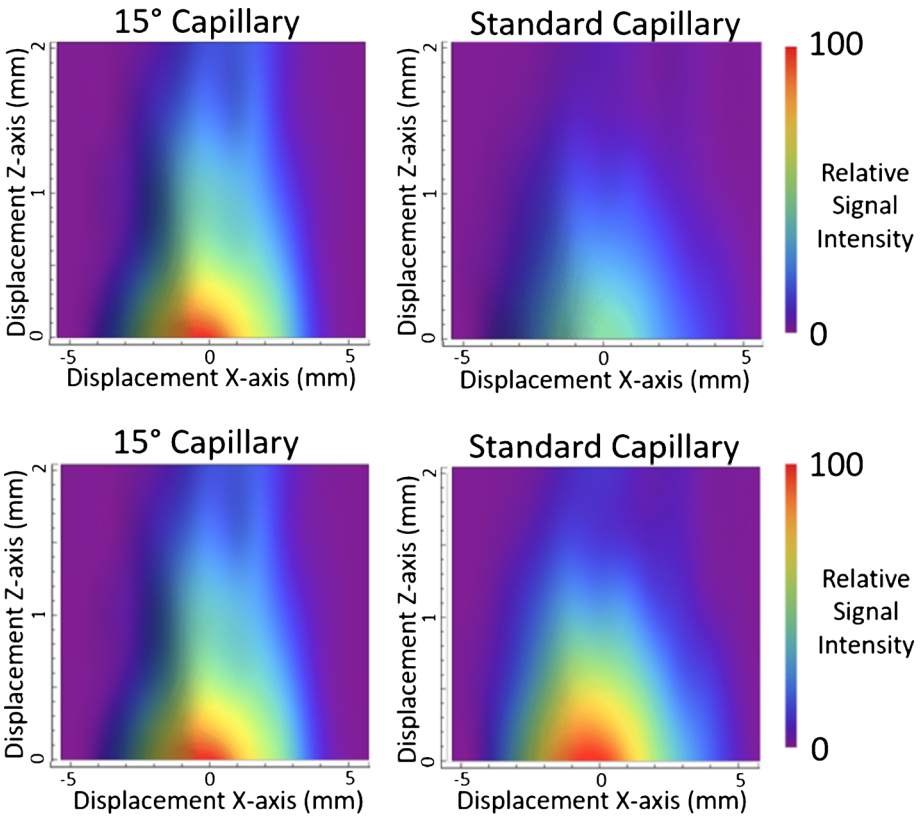

Figure 2. (Top row): each heat map is normalized to the signal intensity at the optimal position for the 15° capillary. (Bottom row): each heat map is normalized individually, and no difference in signal intensity as the emitter is moved from the optimum

dispersion field to the DIMS device. For all experiments conducted with a dispersion field applied, the emitter was kept in the optimal position. Signal intensity was compared at four dispersion fields ranging from 16.0 to 30.0 kV/cm and in transparent mode (Figure 3). For all dispersion fields, the same trend is observed as the experiments where the emitter position was changed. An increase in signal intensity is observed as the angle of the flare decreases. Signal intensity is increased by a factor of 5.5 for the 15° capillary versus the standard capillary. The subsequent loss of signal intensity at the highest dispersion fields is likely due to increased numbers of ions being lost to neutralization at the electrodes when using higher dispersion fields [20, 33].

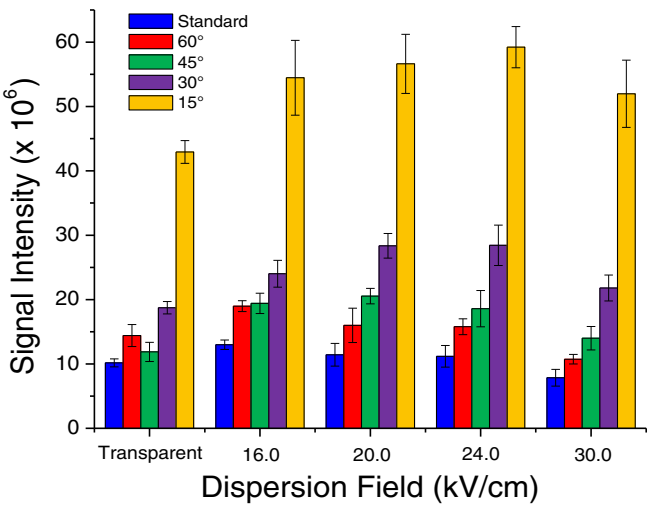

Figure 3. Average signal intensity for the 10+ charge state of lysozyme for each capillary with the DIMS device operated in transparent mode and dispersion fields of 16.0, 20.0, 24.0, and 30.0 V/cm

The 15° capillary was also compared with the standard capillary with and without a DIMS device by summing the signal intensity for all observed charge states of ubiquitin. With either setup (DIMS or no DIMS) the tip of the electrospray emitter was held 4.0 mm from the spray shield. Shorter distances cause electrical discharge between the emitter and spray shield, and any greater distance decreases signal intensity. Without the DIMS device, the 15° capillary and standard capillary show nearly the same signal intensity. This result is consistent with other work on flared capillaries used as atmospheric inlets [34]. However, when a DIMS device is added and operated in transparent mode, the standard capillary shows a 10-fold loss in signal intensity. This loss is reduced to a factor of two when using the 15° capillary. Therefore, although the flared capillaries do not provide increased signal intensity without the DIMS device present for the ESI flow rates used herein, they are useful for increasing the sensitivity of DIMS-MS analyses.

Conclusions

The problem of reduced ion transmission from an atmospheric ion source into the mass spectrometer can be at least partially overcome by flaring the ion-sampling end of the inlet capillary.

Using a flared capillary yields greater signal intensity than the standard capillary when using a DIMS device. This is a simple modification that can be made to any DIMS-MS that uses as inlet capillary to interface the high vacuum to atmosphere, or the flare can be built into the DIMS device [29]. Although the exact mechanism for the increase in signal intensity is not well understood, using flared capillaries does not change the carrier gas conductance through the DIMS device enough to cause any observable changes in separation capabilities. The increase in signal intensity is expected to be a result of sampling a larger area of the sampling slit of the DIMS device. Our experiments also show that increased signal intensity is observed for the flared capillaries even as the emitter is moved from the optimal position, and capillaries with smaller flare angles yield greater increases in absolute signal intensity. It is possible that using even smaller flare angels could further increase ion transmission; however, no other angles were tested due to limitations in machining accurate flare angles into the capillaries.

Acknowledgments

The authors thank Melvin Park, Desmond Kaplan and Mark Ridgeway of Bruker Daltonics for helpful discussions and support of our DIMS project. Bruker Daltonics has licensed certain UNC DIMS IP.

References

1. Shvartsburg, A.A.: Differential Ion Mobility Spectrometry: Nonlinear Ion Transport and Fundamentals of FAIMS. CRC Press, Boca Raton (2009)
2. Eiceman, G.A., Karpas, Z.L.: Ion Mobility Spectrometry, 2nd edn. CRC Press, Boca Raton (2005)
3. Mason, E.A., McDaniel, E.W.: Transport Properties of Ions in Gases. Wiley, New York (1988)
4. Kolakowski, B.M., Mester, Z.: Review of applications of high-field asymmetric waveform ion mobility spectrometry (FAIMS) and differential mobility spectrometry (DMS). Analyst **132**, 842–864 (2007)
5. Hatsis, P., Kapron, J.T.: Review on the application of high-field asymmetric waveform ion mobility spectrometry (FAIMS) in drug discovery. Rapid Commun. Mass Spectrom. **22**, 735–738 (2008)
6. Dharmasiri, U., Isenberg, S.L., Glish, G.L., Armistead, P.M.: Differential Ion mobility spectrometry coupled to tandem mass spectrometry enables targeted leukemia antigen detection. J. Proteome Res. **13**, 4356–4362 (2014)
7. Santiago, B.G., Harris, R.A., Isenberg, S.L., Glish, G.L.: Resolving powers of >7900 using linked scans: how well does resolving power describe the separation capability of differential ion mobility separations. Analyst **140**, 6871–6878 (2015)
8. Bushey, J.M., Kaplan, D.A., Danell, R.M., Glish, G.L.: Pulsed nano-electrospray ionization: characterization of temporal response and implementation with a flared inlet capillary. Instrum. Sci. Tech. **37**, 257–273 (2009)
9. Nazarov, E.G., Coy, S.L., Krylov, E.V., Miller, R.A., Eiceman, G.A.: Pressure effects in differential mobility spectrometry. Anal. Chem. **78**, 7697–7706 (2006)
10. Schneider, B., Covey, T., Coy, S., Krylov, E., Nazarov, E.: Chemical effects in the separation process of a differential mobility/mass spectrometer system. Anal. Chem. **82**, 1867–1880 (2010)
11. Barnett, D.A., Belford, M., Dunyach, J.J., Purves, R.W.: Characterization of a temperature-controlled FAIMS system. J. Am. Soc. Mass Spectrom. **18**, 1653–1663 (2007)
12. Wilks, A., Hart, M., Koehl, A., Somerville, J., Boyle, B., Ruiz-Alonso, D.: Characterization of a miniature, ultra-high-field, ion mobility spectrometer. Int. J. Ion Mobility Spectrom. **15**, 199–222 (2012)
13. Purves, R.W., Guevremont, R., Day, S., Pipich, C.W., Matyjaszczyk, M.S.: Mass spectrometric characterization of a high-field asymmetric waveform ion mobility spectrometer. Rev. Sci. Instrum. **69**, 4094–4105 (1998)
14. Buryakov, I., Krylov, E., Nazarov, E., Rasulev, U.: A new method of separation of multi-atomic ions by mobility at atmospheric pressure using a high-frequency amplitude-asymmetric strong electric field. Int. J. Mass Spectrom. Ion Processes **128**, 143–148 (1993)
15. Guevremont, R., Purves, R.W., Barnett, D.A., Ding, L.Y.: Ion trapping at atmospheric pressure (760 Torr) and room temperature with a high-field asymmetric waveform ion mobility spectrometer. Int. J. Mass Spectrom. **193**, 45–56 (1999)
16. Guevremont, R., Purves, R.W.: High field asymmetric waveform ion mobility spectrometry-mass spectrometry: an investigation of leucine enkephalin ions produced by electrospray ionization. J. Am. Soc. Mass Spectrom. **10**, 492–501 (1999)
17. Guevremont, R., Purves, R.W.: Atmospheric pressure ion focusing in a high-field asymmetric waveform ion mobility spectrometer. Rev. Sci. Instrum. **70**, 1370–1383 (1999)
18. Barnett, D.A., Ells, B., Guevremont, R., Purves, R.W.: Separation of leucine and isoleucine by electrospray ionization-high field asymmetric waveform ion mobility spectrometry-mass spectrometry. J. Am. Soc. Mass Spectrom. **10**, 1279–1284 (1999)
19. Purves, R., Guevremont, R.: Electrospray ionization high-field asymmetric waveform ion mobility spectrometry-mass spectrometry. Anal. Chem. **71**, 2346–2357 (1999)
20. Shvartsburg, A.A., Ibrahim, Y.M., Smith, R.D.: Differential ion mobility separations in up to 100% helium using microchips. J. Am. Soc. Mass Spectrom. **25**, 480–489 (2014)
21. Shvartsburg, A.A., Tang, K.Q., Smith, R.D., Holden, M., Rush, M., Thompson, A., Toutoungi, D.: Ultrafast differential ion mobility spectrometry at extreme electric fields coupled to mass spectrometry. Anal. Chem. **81**, 8048–8053 (2009)
22. Page, J.S., Kelly, R.T., Tang, K., Smith, R.D.: Ionization and transmission efficiency in an electrospray ionization-mass spectrometry interface. J. Am. Soc. Mass Spectrom. **18**, 1582–1590 (2007)
23. Davis, D., Portelius, E., Zhu, Y., Feigerle, C., Cook, K.D.: Profiling an electrospray plume using surface-enhanced Raman spectroscopy. Anal. Chem. **77**, 8151 (2005)
24. Girod, M., Dagany, X., Boutou, V., Broyer, M., Antoine, R., Dugourd, P., Mordehai, A., Love, C., Werlich, M., Fjeldsted, J., Stafford, G.: Profiling an electrospray plume by laser-induced fluorescence and fraunhofer diffraction combined to mass spectrometry: influence of size and composition of droplets on charge-state distributions of electrosprayed proteins. Phys. Chem., Chem. Phys. **14**, 9389 (2012)
25. Krutchinsky, A.N., Padovan, J.C., Cohen, H., Chait, B.T.: Maximizing ion transmission from atmospheric pressure into the vacuum of mass spectrometers with a novel electrospray interface. J. Am. Soc Mass Spectrom. **26**, 649–658 (2015)
26. Prasad, S., Wouters, E.R., Dunyach, J.: Advancement of atmospheric-vacuum interfaces for mass spectrometers with a focus on increasing gas throughput for improving sensitivity. Anal. Chem. **87**, 8234–8241 (2015)
27. Shvartsburg, A.A., Smith, R.D.: Scaling of the resolving power and sensitivity for planar FAIMS and mobility-based discrimination in flow- and field-driven analyzers. J. Am. Soc. Mass Spectrom. **18**, 1672–1681 (2007)
28. Tang, K., Shvartsburg, A.A., Smith, R.D.: Interface and process for enhanced transmission of non-circular ion beams between stages at unequal pressure. US Patent Number 7,339,166. US 11/361,264 (2008)
29. Isenberg, S.L., Armistead, P.M., Glish, G.L.: Optimization of peptide separations by differential ion mobility spectrometry. J. Am. Soc. Mass Spectrom. **25**, 1592–1599 (2014)
30. Shvartsburg, A.A., Smith, R.D.: Ultrahigh-resolution differential ion mobility spectrometry using extended separation times. Anal. Chem. **83**, 23–29 (2011)
31. Krylov, E.V., Coy, S.L., Vandermey, J., Schneider, B.B., Covey, T.R., Nazarov, E.G.: Selection and generation of waveforms for differential mobility spectrometry. Rev. Sci. Instrum. **81**, 024101-1-11 (2010)
32. Glish, G.L., Danell, R.M.: Electrospray ionization device. US Patent No. 6,703,611 (2004)
33. Shvartsburg, A.A., Smith, R.D., Wilks, A., Koehl, A., Ruiz-Alonso, D., Boyle, B.: Ultrafast differential ion mobility spectrometry at extreme electric fields in multichannel microchips. Anal. Chem. **81**, 6489–6495 (2009)
34. Dixon, R.B., Muddiman, D.C.: Quantitative comparison of a flared and a standard heated metal capillary inlet with a voltage-assisted air amplifier on an electrospray ionization linear ion trap mass spectrometer. Rapid Commun. Mass Spectrom. **21**, 3207–3212 (2007)